J. Fluid Mech. (2002), *vol.* 473, *pp.* 147–166. © 2002 Cambridge University Press
DOI: 10.1017/S0022112002002318 Printed in the United Kingdom

Resonance forever: existence of a critical mass and an infinite regime of resonance in vortex-induced vibration

By R. GOVARDHAN† AND C. H. K. WILLIAMSON

Sibley School of Mechanical and Aerospace Engineering, Upson Hall, Cornell University, Ithaca, NY 14853-7501, USA

(Received 5 March 2002 and in revised form 8 July 2002)

In this paper, we study the transverse vortex-induced vibrations of a cylinder with no structural restoring force ($k = 0$). In terms of the conventionally used normalized flow velocity, U^*, the present experiments correspond to an infinite value (where $U^* = U/f_N D$, f_N = natural frequency, D = diameter). A reduction of mass ratios m^* (mass/displaced mass) from the classically studied values of order $m^* = 100$, down to $m^* = 1$, yields negligible oscillations. However, a further reduction in mass exhibits a surprising result: large-amplitude vigorous vibrations suddenly appear for values of mass less than a *critical mass ratio*, $m^*_{crit} = 0.54$. The classical assumption, since the work of den Hartog (1934), has been that resonant large-amplitude oscillations exist only over a narrow range of velocities, around $U^* \sim 5$, where the vortex shedding frequency is comparable with the natural frequency. However, in the present study, we demonstrate that, so long as the body's mass is below this critical value, the regime of normalized velocities (U^*) for resonant oscillations is infinitely wide, beginning at around $U^* \sim 5$ and extending to $U^* \to \infty$. This result is in precise accordance with the predictions put forward by Govardhan & Williamson (2000), based on elastically mounted vibration studies (where $k > 0$). We deduce a condition under which this unusual concept of an infinitely wide regime of resonance will occur in any generic vortex-induced vibration system.

1. Introduction and preliminary results

The problem of vortex-induced vibration of structures, in particular the case where a rigid circular cylinder is elastically mounted and constrained to oscillate transversely to a free stream, has been well-studied in the literature, as may be seen, for example, from the comprehensive reviews of Sarpkaya (1979), Bearman (1984) and Parkinson (1989). However, there have been almost no previous investigations of such a system in the limiting case where there is no structural restoring force, i.e. in the absence of any attached springs. We shall show that the results of such an investigation have important implications for an elastically mounted body. The only work that does exist in the literature along these lines, is the low Reynolds number ($Re = 100$) computational study of Shiels, Leonard & Roshko (2001). In the present paper, we have manipulated their data and we deduce results qualitatively in good accordance with the present experimental results. The range of Reynolds numbers for the present experimental study is from $Re = 4000$ to $Re = 22\,000$.

† Present address: Aerospace Engineering Department, Indian Institute of Technology – Madras, Chennai 600036, India.

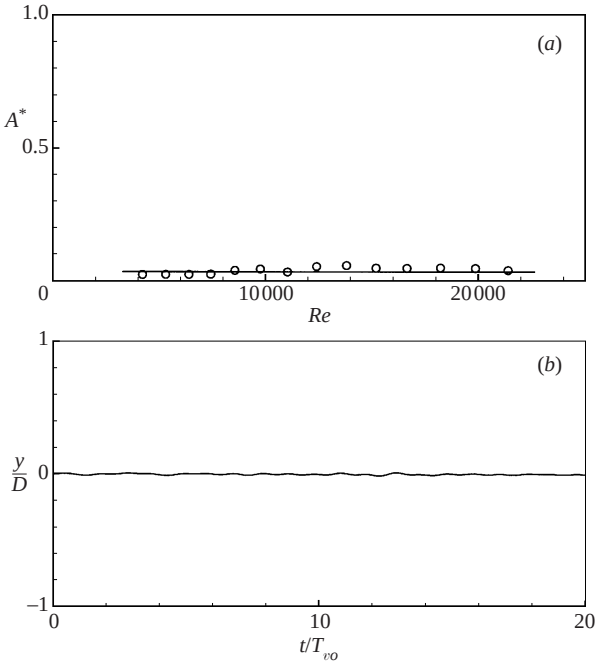

FIGURE 1. (*a*) Response of a cylinder with no springs for $m^* = 1.67$, showing the absence of any significant oscillations ($A^* = A/D$), over a range of flow speeds. Normalized frequency (fD/U), of the very small oscillations, remains near the Strouhal number ($S = 0.2$), as flow speed is varied. (*b*) An example time trace at $Re \approx 5100$.

We began this study with a cylinder which had a very low mass ratio, $m^* = 1.67$ (m^* = oscillating mass/displaced fluid mass), and were immediately intrigued by its response, which is shown in figure 1. Despite the fact that one could move the cylinder, mounted on air-bearings, simply by brushing it with a feather, we found that, over a large range of flow speeds, the body remained essentially stationary. This was surprising to us given that the cylinder is completely free to move transverse to the flow, and is subjected to large transverse (lift) forces, as may be inferred from the strong periodic shedding of vortices shown in figure 2(*a*). It should also be noted here that the structural damping of our air-bearing system is extremely low, as discussed in § 2.

Simply by reducing the mass ratio to $m^* = 0.45$, we discovered that large-amplitude oscillations occured. These vigorous oscillations (in figure 3) were at amplitudes of the order of $A^* = A/D \approx 0.80$, where D is cylinder diameter, and remained independent of flow speed over the wide range of flow velocities (or Reynolds numbers) investigated. This huge change in the dynamics of the cylinder, from essentially no oscillations to a system with large-amplitude vibrations, triggered by only a small change in mass ratio, suggests the possibility that there could exist a *critical mass ratio* at which there is a sudden 'catastrophic' change in the body dynamics. We therefore study the existence of such a critical mass ratio in § 3.

It is also interesting to note that the wake vortex dynamics for the case that exhibits large oscillations, shown in figure 2(*b*), is quite different from that in figure 2(*a*) for the nearly stationary cylinder case, and indicates a '2P' wake mode (as defined by Williamson & Roshko 1988) with two counter-rotating vortex pairs being shed per oscillation cycle. In this case, the second vortex of each pair is relatively weak

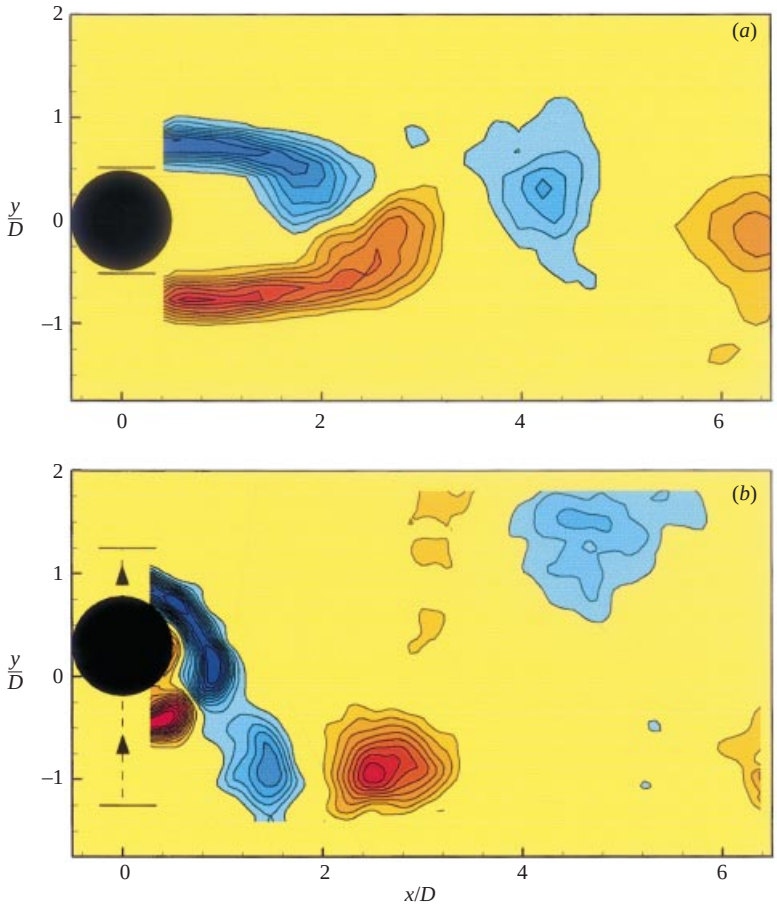

FIGURE 2. Vorticity plots from DPIV, for a cylinder vibrating without springs: (*a*) the 2S wake mode at $m^* = 1.67$, and (*b*) the 2P mode at $m^* = 0.45$. In (*b*), two vortex pairs are formed per cycle, although the second vortex of each pair is much weaker than the first, and decays rapidly. Blue contours show clockwise vorticity, red anticlockwise vorticity. Contour levels shown are $\omega D/U = \pm 0.5, \pm 1.0, \pm 1.5 \ldots$. $Re \approx 5100$ in both cases.

compared to the first vortex of the pair, and decays rapidly; this pattern is quite reminiscent of the wake vortex pattern found in the 'upper' branch of amplitude response in Govardhan & Williamson (2000), for a spring-mounted cylinder.

For each case discussed above, the ratio of the stationary-body shedding frequency (f_{vo}) to the actual oscillation frequency (f) remained nearly constant with flow speed ($Re = 4000$–$20\,000$). However, the value of the constant depends on the mass ratio. For the very small mass ($m^* = 0.45$), we find $(f_{vo}/f) = 1.21 \pm 0.03$. For the $m^* = 1.67$ case, we find $(f_{vo}/f) \approx 1.0$.

Since both the response amplitude and the oscillation frequency ratio (f_{vo}/f) are nearly independent of flow speed (if mass ratio is fixed), it would be useful to see these responses in a frequency–amplitude plane of the type used in the elastically mounted body studies of Khalak & Williamson (1999) and Govardhan & Williamson (2000). The most fundamental frequency parameter will depend on the actual oscillation frequency (f) and the vortex shedding frequency in the absence of oscillations (f_{vo}), under otherwise similar conditions. The frequency ratio (f_{vo}/f) can be shown to be

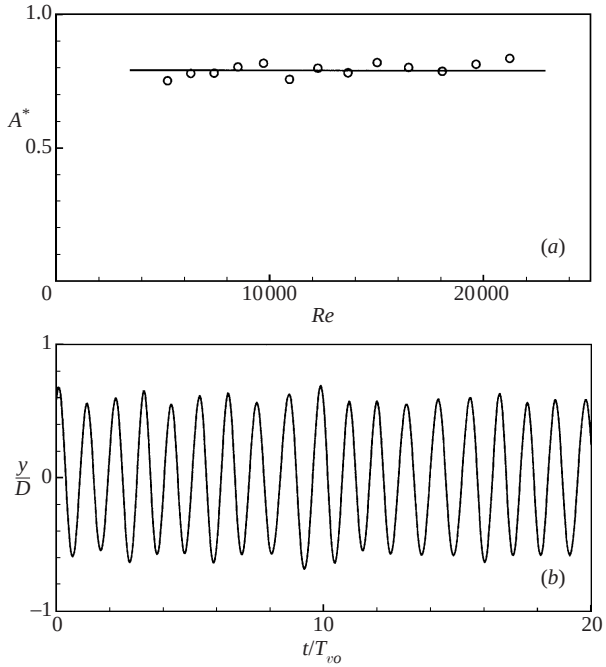

FIGURE 3. (*a*) Response of a cylinder with no springs for $m^* = 0.45$, showing large-amplitude oscillations ($A^* = A/D \approx 0.8$), over a range of flow speeds. Normalized frequency (fD/U) is significantly different from the Strouhal number ($S = 0.2$), but remains at nearly a constant value, as flow speed is varied. (*b*) An example time trace at $Re \approx 5100$.

$(U^*/f^*)S$, using the parameters employed in Khalak & Williamson (1999) (where $U^* = U/f_N D$; $f^* = f/f_N$; U = flow velocity; f_N = structural natural frequency; S = Strouhal number). In the present experiments with no springs, the spring constant k, as well as the structural natural frequency (for the body in vaccuo) $f_N = 1/2\pi\sqrt{k/m}$, are both zero. Therefore, both U^* and f^* are infinite, as indicated for clarity below:

$$k = 0: \quad U^* = \frac{U}{f_N D} = \infty \quad \text{(for any } U\text{)},$$

$$k = 0: \quad f^* = \frac{f}{f_N} = \infty \qquad \text{(for any } f\text{)}.$$

On the other hand, the parameter $(U^*/f^*)S = (f_{vo}/f)$ does indeed remain finite, since both the actual cylinder oscillation frequency (f) and the stationary-body vortex shedding frequency (f_{vo}) are non-zero and finite. Hence, the oscillations for the present $k = 0$ experiments lie in the finite $\{(f_{vo}/f), A^*\}$ plane, as may be seen in figure 4. Also, it is clear from this figure that the response in this plane is nearly independent of flow speed (the data points for all the different flow speeds of figures 1 and 3 collapse onto the same point, as expected from the almost constant values of (f_{vo}/f) and A^*). We shall refer to this response point on the frequency–amplitude plane as the '*operating point*', and we will discuss it in more detail in §4. It may also be seen from figure 4 that the '2P mode' wake dynamics for the oscillating case (figure 2*b*), corresponds well with the map of wake modes in the frequency–amplitude plane found from forced vibration experiments (Williamson & Roshko 1988).

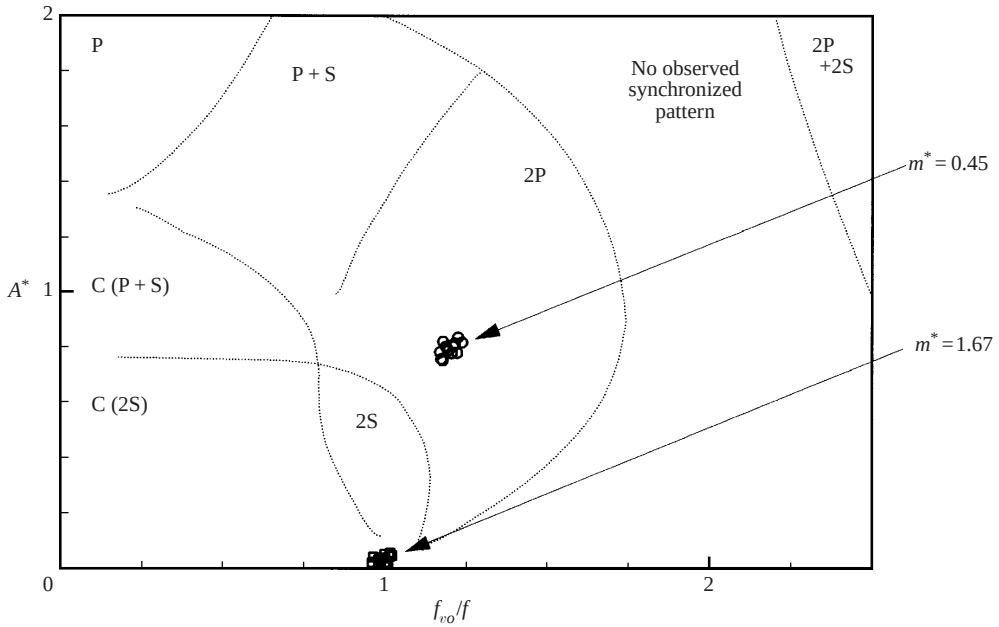

FIGURE 4. Response data of figures 1 and 3 on the frequency–amplitude plane $\{f_{vo}/f, A^*\}$, indicating that the oscillations are essentially independent of flow speed, in this plane. f_{vo} is the vortex shedding frequency in the absence of body oscillations, and f is the actual cylinder oscillation frequency. □, $m^* = 1.67$; ○, $m^* = 0.45$; ···, Williamson & Roshko (1988) map of wake modes from forced vibration studies.

We shall now set out to explain the intriguing result that the body with larger mass does not vibrate, while the slightly lighter body exhibits vigorous large-amplitude oscillations.

2. Experimental details

The present experiments were conducted using a hydroelastic facility, which is described in detail in Khalak & Williamson (1996, 1999), in conjunction with the Cornell-ONR Water Channel. The hydroelastic facility comprises air-bearings mounted above the channel test section, which allow a vertical cylinder in the fluid to move transverse to the free stream. The use of air-bearings leads to an extremely small structural damping, as characterized in the Appendix. The turbulence level in the test section of the Water Channel was less than 0.9%, in the 15 in. × 20 in. (0.381 m × 0.508 m) cross-section, over the range of free-stream velocities U (0.04–0.32 m s^{-1}) used in this study. The test cylinder had a diameter of 0.0794 m, and a length–diameter ratio of 6. In the absence of restraining springs in the experimental arrangement, and over sufficiently long times (> 10 minutes), the body could deviate very slowly (by random walk) from its original location by a diameter or so, and therefore careful zeroing of the data was necessary at the time of taking measurements.

For the purpose of employing DPIV, the flow was seeded with 14-micron silver-coated glass spheres, which were illuminated by a sheet of laser light from a 5 W Argon ion laser. Pairs of particle images were captured using a high-resolution CCD Kodak Megaplus (1008 × 1018 pixels) camera, and analysed using cross-correlation of sub-images, our implementation of which is described in more detail in Govardhan & Williamson (2000). The resulting DPIV vorticity fields were phase averaged (over 10 cycles) using cylinder position as a reference. This process will yield the averaged

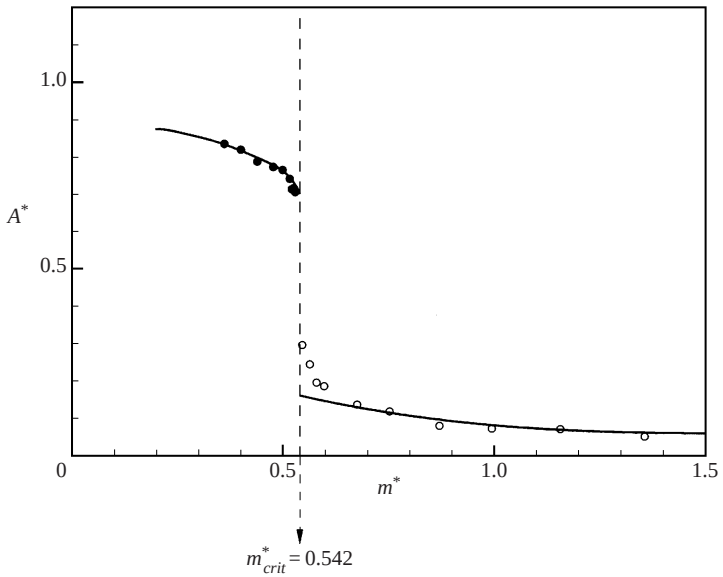

FIGURE 5. Existence of a critical mass. Amplitude response (A^*) as mass ratio (m^*) is decreased, showing the sudden appearance of large-amplitude oscillations for m^* less than a critical value (m^*_{crit}) of 0.542. ●, $m^* < m^*_{crit}$; ○, $m^* > m^*_{crit}$.

primary vorticity field that is parallel with the body, without the apparent effects due to small-scale three-dimensionality, which are present in individual images. There is a slight thickening (around 10%) of the separating shear layers close to the body from the averaging process, and the resulting vorticity images are quite comparable with the photographic PIV measurements from forced vibration studies in Carberry *et al.* (2002). The origin of the coordinate system is fixed at the position of the cylinder, at zero flow speed. The x-axis is downstream, the y-axis is perpendicular to the flow direction and to the cylinder axis (defined as transverse), and the z-axis lies along the axis of the cylinder.

3. Existence of a critical mass

As described in the Introduction (§ 1), the cylinder remained stationary for mass ratio $m^* = 1.67$, but exhibited vigorous large-amplitude oscillations for the $m^* = 0.45$ case. Keeping this result in mind, we then reduced the mass ratio m^* in small steps from the larger m^* value, down to $m^* \approx 0.30$. The corresponding response amplitudes are shown in figure 5. It is clear that there is a sudden transition from the no-oscillation state to a state where there are large-amplitude oscillations at a *critical mass ratio*,

$$m^*_{crit} = 0.542 \pm 0.01. \tag{3.1}$$

For $m^* > m^*_{crit}$, the cylinder is almost stationary, while for $m^* < m^*_{crit}$, the cylinder exhibits large-amplitude oscillations. This existence of a critical mass is a central result of the present paper.

The oscillation frequency also shows a sudden change as the mass ratio decreases below the critical value, $m^*_{crit} = 0.54$, as one might suspect. The effect of this combined large change in frequency and amplitude is a huge jump in the location of the 'operating point', as may be seen in figure 6. It should be noted that for $m^* > m^*_{crit}$, the

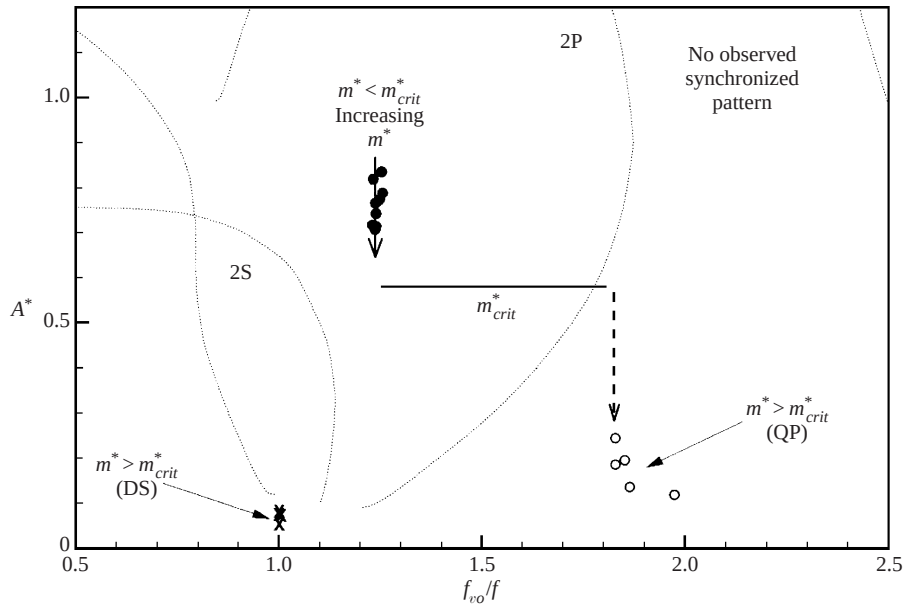

FIGURE 6. Location of the 'operating point' in the frequency–amplitude plane, as the mass ratio is increased. ●, $m^* < m^*_{crit}$; ○, $m^* > m^*_{crit}$ where the vibrations are quasi-periodic (QP); ×, $m^* > m^*_{crit}$ where the vibrations are desynchronized (DS).

oscillations are very small and, therefore, the body is not able to keep the wake vortex dynamics synchronized to its motions. This leads to either quasi-periodic oscillations (denoted as QP on the figure), for mass ratios that are only slightly larger than m^*_{crit}, or desynchronized, almost negligible, oscillations (denoted as DS), for m^* reasonably larger than m^*_{crit}. In the completely desynchronized case, the oscillation frequency (as can be detected even at almost negligible amplitudes) is at the vortex-shedding frequency corresponding to the non-oscillating body (f_{vo}), so that $f_{vo}/f \approx 1.0$, as found earlier for the $m^* = 1.67$ case.

In the following section, we shall look at the equation of motion governing the body dynamics, which holds the key to the location of the Operating Point in the frequency–amplitude plane, and hence to an understanding of the critical mass ratio.

4. An 'operating point' in the frequency–amplitude plane

For the present experiments with no springs, the oscillation amplitude (A^*) and frequency ratio (f_{vo}/f) are nearly independent of flow speed, at a fixed value of mass ratio. There is therefore a collapse of the response data (over all the flow speeds) to a single point in the frequency–amplitude plane. We define this response point in the frequency–amplitude plane to be the '*operating point*' for the system (using terminology similar to that used in turbomachinery text books to describe the state of a compressor or turbine in the mass-flow–pressure ratio plane).

As the mass ratio (m^*) is varied, the location of the operating point in the frequency–amplitude plane changes, as shown in figure 6. This leads to the question: *What determines the location of the operating point?* In order to answer this, we shall look at the equation of motion for the cylinder.

The equation of motion which represents the vortex-induced vibrations of a cylinder

in the transverse y-direction with no attached springs, may be written as

$$m\ddot{y} + c\dot{y} = F, \tag{4.1}$$

where $m =$ total oscillating structural mass, $c =$ structural damping and $F =$ fluid force in the transverse direction. When the body oscillation frequency is synchronized with the periodic vortex wake mode, the force and displacement are very well predicted by sinusoidal functions:

$$F(t) = F_o \sin(\omega t + \phi), \tag{4.2}$$

$$y(t) = A \sin(\omega t), \tag{4.3}$$

where $\omega = 2\pi f$ and $\phi =$ phase angle between the fluid force and the body displacement.

4.1. *Amplitude equation*

An equation for the response amplitude can be derived in a straightforward manner, by substituting equations (4.2)–(4.3) into equation (4.1) and balancing $\cos(\omega t)$ terms, in a manner similar to what is done for an elastically mounted cylinder (see Khalak & Williamson 1999, for example):

$$cA\omega = F_o \sin\phi. \tag{4.4}$$

Re-arranging the above equation, and normalizing the force (F_o) by ($\frac{1}{2}\rho U^2 DL$) to give C_y, and normalizing the oscillating mass (m) by the displaced fluid mass ($\pi\rho D^2 L/4$) to give m^* ($\rho =$ fluid density, $L =$ cylinder length, $D =$ diameter), we may write

$$A^* = \frac{1}{4\pi^3} \frac{C_y \sin\phi}{(m^* + C_A)} \left(\frac{f_{vo}}{f}\right) \frac{1}{S^2} \Big/ \left[\frac{c}{4\pi f_{vo}(m + m_A)}\right], \tag{4.5}$$

where C_A is the potential added-mass coefficient ($C_A = 1.0$ for a circular cylinder), $m_A = C_A \pi\rho D^2 L/4$ and $S =$ Strouhal number $= f_{vo} D/U$. The non-dimensional damping parameter in the above equation (within square brackets) may be defined as an equivalent damping ratio (ζ_{eq}), as discussed in more detail in the Appendix, thus making the amplitude equation

$$A^* = \frac{1}{4\pi^3} \frac{C_y \sin\phi}{(m^* + C_A)\zeta_{eq}} \left(\frac{f_{vo}}{f}\right) \frac{1}{S^2}. \tag{4.6}$$

(The combined mass-damping parameter, $(m^* + C_A)\zeta_{eq}$, may in turn be defined to be the 'equivalent mass-damping'.) This amplitude equation is a statement of energy balance, i.e. energy transferred from fluid excitation to body motion (proportional to $C_y \sin\phi$) is equal to the energy lost due to damping, over a cycle.

4.2. *'Frequency' equation*

In the case of a finite spring constant ($k > 0$), the equation that results from a balance of the ($\sin\omega t$) terms yields the frequency, and so we shall label the resulting equation, even in the case of zero spring stiffness ($k = 0$) as the 'frequency' equation. The 'frequency' equation is key to understanding the location of the operating point. We shall show the equations step by step, for the purpose of clarity, as follows:

$$\begin{aligned} m\ddot{y} + c\dot{y} &= F_o \sin(\omega t + \phi) \\ &= \underbrace{(F_o \cos\phi)\sin(\omega t)}_{\left[\begin{array}{c}\text{in phase with acceleration}\\ \ddot{y} = -A\omega^2 \sin(\omega t)\end{array}\right]} + \underbrace{(F_o \sin\phi)\cos(\omega t).}_{\left[\begin{array}{c}\text{in phase with velocity}\\ \dot{y} = A\omega \cos(\omega t)\end{array}\right]} \end{aligned}$$

The part of the lift force in phase with acceleration ($\ddot{y}$) may be thought of as an 'effective added mass' force, where the effective added mass (m_{EA}) is given by

$$m_{EA} = \frac{\text{Effective added mass force}}{\text{acceleration}} = \frac{F_o \cos\phi}{A\omega^2}. \tag{4.7}$$

For the purpose of clarity in the present derivation, this effective added mass can be absorbed into the inertia term on the left, giving

$$\underbrace{(m + m_{EA})\ddot{y}}_{\sin\omega t} + \underbrace{c\dot{y}}_{\cos\omega t} = \underbrace{(F_o \sin\phi)\cos(\omega t)}_{\cos\omega t}. \tag{4.8}$$

Balancing the $\sin\omega t$ terms in the above equation implies that the coefficient of the first term needs to be zero, which after non-dimensionalizing by the displaced fluid mass ($\pi\rho D^2 L/4$) gives the simple, but important, 'frequency' equation:

$$m^* + C_{EA} = 0, \tag{4.9}$$

where C_{EA} is the effective added mass coefficient defined as

$$C_{EA} = \frac{m_{EA}}{\pi\rho D^2 L/4} = \frac{1}{2\pi^3 A^* S^2}\left(\frac{f_{vo}}{f}\right)^2 C_y \cos\phi. \tag{4.10}$$

4.3. *Location of the operating point*

In the frequency–amplitude plane (for a given structural mass and damping), there exists a set of points satisfying the amplitude equation (equation (4.6)), and another set of points that satisfy the frequency equation (equation (4.9)). At the operating point, both the amplitude and frequency equations would have to be satisfied. Therefore, the operating point will be located at the intersection of the two sets of points.

In order to illustrate this, let us consider for example the case where damping $c = 0$ and $m^* = 0.4$. From the amplitude equation (4.4), $c = 0$ would imply that the fluid excitation ($F_o \sin\phi$) or ($C_y \sin\phi$) should also be zero, and so we seek the contour in the frequency–amplitude plane for which there is zero excitation. The forced vibration experiments of Gopalkrishanan (1993) and Hover, Techet & Triantafyllou (1998), where the cylinder is forced to oscillate at different amplitudes and frequencies, gives us some idea of the shape of this 'zero-excitation' contour in the frequency–amplitude plane, and is shown schematically in figure 7. One can also measure, from forced vibration experiments, the contour in the frequency–amplitude plane for which $C_{EA} = -0.4$, thereby satisfying the frequency equation, $C_{EA} = -m^*$. The operating point would therefore be at the intersection of these two contours as indicated in figure 7. This is the only location in the frequency–amplitude plane, where both the amplitude and frequency equations are satisfied in this case.

The above concepts are valid even for non-zero damping. In general, as the damping is increased (for the same m^*), the operating point would move to lower amplitudes on the $C_{EA} = -m^*$ contour.

5. Critical mass

In this section, we shall use the concept of the operating point to understand the existence of the critical mass.

In the absence of springs the position of the operating point depends very sensitively on the mass ratio, m^* (for a given structural damping). This is clear from the frequency

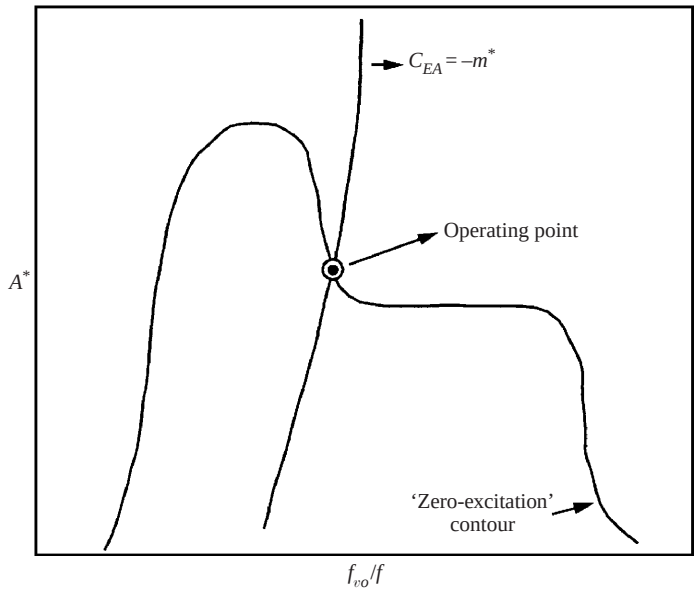

FIGURE 7. Schematic showing the location of the 'operating point' at the intersection of the curves representing the points satisfying the amplitude equation ('zero-excitation' contour) and frequency equation ($C_{EA} = -m^*$), for a system with no springs ($k = 0$) and zero structural damping ($c = 0$).

equation (4.9), which we recall is

$$-C_{EA} = m^*.$$

The effective added mass coefficient, C_{EA}, depends on the magnitude of the fluid force coefficient (C_y) and the phase angle (ϕ) between C_y and the body displacement, as shown in equation (4.10). The numerical value of C_{EA} is defined by the wake vortex dynamics.

We now address the question: Under what conditions will the cylinder vibrate? Let us continue to use the example in figure 7, where $c = 0$ and $k = 0$. The answer to the question posed above is completely decided by whether the wake vortex dynamics can yield a value of C_{EA}, somewhere along the non-negligible amplitude curve (see the zero-excitation curve in figure 7), which can physically satisfy equation (4.9). Therefore, for a given mass ratio, m^*, and along the non-negligible amplitude curve:

if wake vortex dynamics can satisfy: $-C_{EA} = m^*$
then the body will vibrate;
if wake vortex dynamics cannot satisfy: $-C_{EA} = m^*$
then the body will NOT vibrate.

This leads to the question: *What is the numerical range of m^* to allow vibration?* To answer this question, let us look at a typical $[-C_{EA}]$ data set, from the spring-mounted ($k > 0$) experiments in Govardhan & Williamson (2000), as shown in figure 8. It can clearly be seen from the figure that the wake dynamics can provide values of $[-C_{EA}]$ up to a maximum of $[-C_{EA}]_{max} = 0.54$, which occurs in the 'lower' response branch (response branches such as in the lower plot of figure 8 are described in detail in Govardhan & Williamson 2000). Further experiments and discussion in Govardhan & Williamson (2000) indicate that the value of $[-C_{EA}]$ on the lower branch is

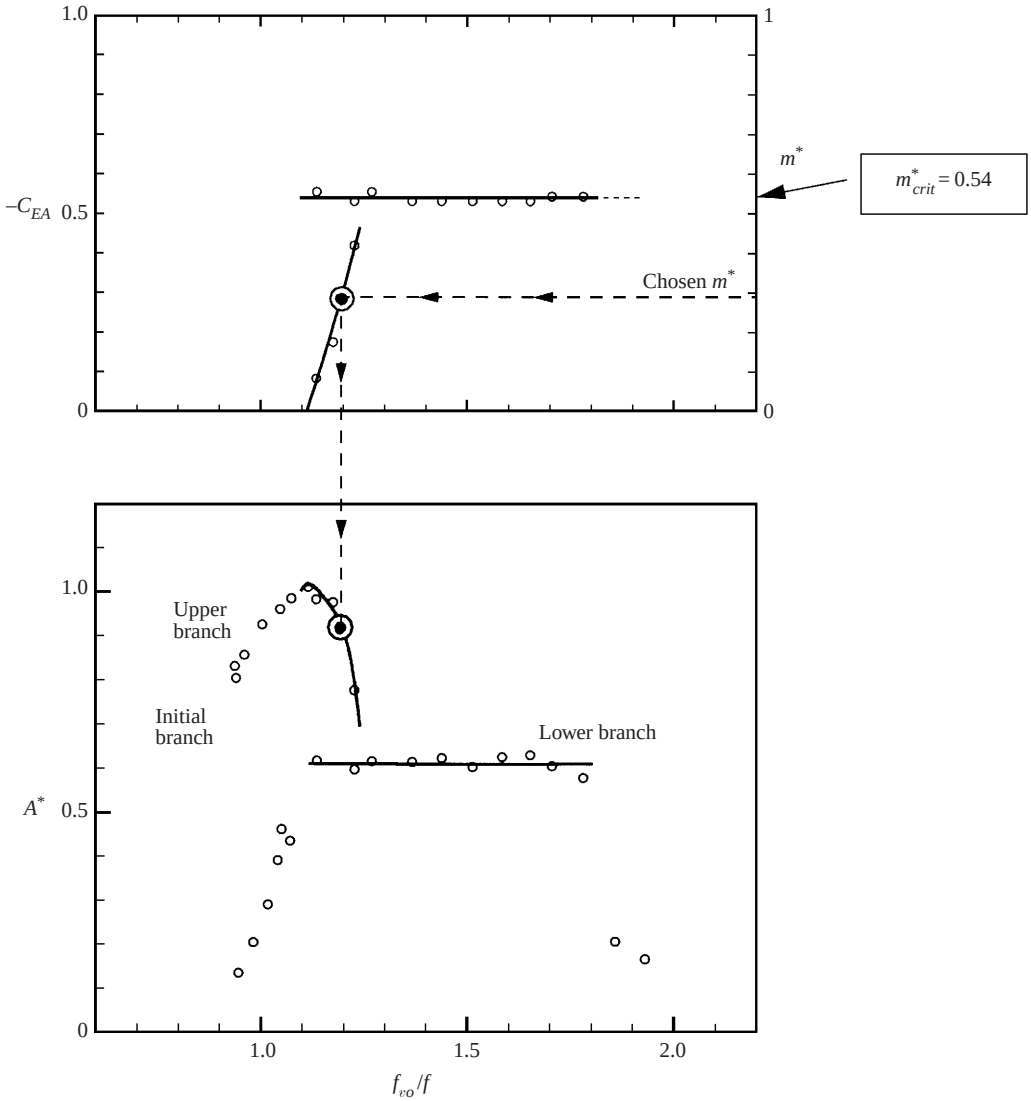

FIGURE 8. Prediction of possible response amplitudes at $k = 0$, from $k > 0$ response measurements in Govardhan & Williamson (2000). The frequency condition for $k = 0$ experiments, $m^* = -C_{EA}$, dictates the oscillation amplitude ($\odot$) at any chosen m^* (or equivalently $-C_{EA}$), as illustrated above. For $m^* > [-C_{EA}]_{max} = 0.54$, the frequency condition cannot be satisfied for any synchronized oscillations, and therefore the cylinder stops vibrating. $\bigcirc$, $k > 0$ response data from Govardhan & Williamson (2000) ($m^* = 1.19$ and $\zeta = 0.005$).

independent of mass and damping, as long as the combined mass-damping parameter is reasonably small $[(m^* + C_A)\zeta < 0.1]$. Therefore, the result $[-C_{EA}]_{max} = 0.54$ holds accurately for such vibrating systems, under these conditions of small mass-damping.

The above discussion implies that for a cylinder in the absence of springs ($k = 0$) and with small values of mass-damping, the body can vibrate only if the chosen mass ratio, m^*, is less than 0.54, thus indicating the existence of a critical mass ratio, m^*_{crit}. The value of critical mass has now been found from the study of Govardhan & Williamson (2000) (for $k > 0$), and also from the present experiments (for $k = 0$). We

find a remarkable numerical agreement of m^*_{crit} as follows:

$$m^*_{crit} = [-C_{EA}]_{max} = 0.54 \pm 0.02 \tag{5.1}$$

(from $k > 0$ experiments; Govardhan & Williamson 2000),

$$m^*_{crit} = 0.542 \pm 0.01 \tag{5.2}$$

(from $k = 0$ experiments; present results).

6. Infinite regime of resonance

We have looked so far at the critical mass ratio in experiments without springs (spring constant, $k = 0$), which as discussed in the Introduction corresponds to normalized flow velocity $U^* = U/f_N D = \infty$. From the primary result of this paper in figure 5 where large-amplitude vibration is found for $m^* < m^*_{crit}$, we therefore have the result that 'resonant' oscillations exist even at infinite normalized velocity, U^*, when $m^* < m^*_{crit}$. This proves the prediction of Govardhan & Williamson (2000) that large-amplitude oscillations can exist up to infinite normalized velocities, as indicated by their equation (6.5):

$$U^*_{end} \approx 9.25\sqrt{\frac{(m^* + C_A)}{(m^* - 0.54)}} \to \infty \quad \text{as} \quad m^* \to m^*_{crit} = 0.54.$$

This equation shows that the value of U^* marking the end of the large-amplitude synchronization regime (U^*_{end}) extends to infinity as $m^* \to m^*_{crit}$.

Under these conditions, the regime of resonance extends over an infinitely wide range of U^*, and in this sense the cylinder resonates forever!

We illustrate such an infinitely wide regime of resonance for the particular case $m^* = 0.52$ (so that $m^* < m^*_{crit}$), and for $k > 0$, in figure 9. We include also the response at $U^* = \infty$, from the $k = 0$ experiments. It may also be seen that the frequency response $f^* = f/f_N$ increases continuously with U^*, reaching large values, while C_{EA} asymptotes towards the condition $C_{EA} = -m^*$, as $U^* \to \infty$.

A striking feature of any $m^* < m^*_{crit}$ response, as may be seen from figure 9, is the fact that there exist 'resonant' large-amplitude oscillations even when the oscillation frequency (f) is large compared to the natural frequency (f_N). For example, from the nearly linear variation of $f^* = f/f_N$ in figure 9, we can deduce that at,

$$U^* = 500: \quad f \approx 87 f_N,$$
$$U^* = 1000: \quad f \approx 174 f_N.$$

This is very far from the classical expectation of large-amplitude response only when $f \approx f_N$. This raises the important question: How is it possible to have large-amplitude oscillations when $f \gg f_N$?

In order to understand this phenomenon in simple terms, let us now look at a straightforward forced linear oscillator, noting that this is the generic type of equation of motion usually employed for bodies undergoing vortex-induced vibration:

$$m\ddot{y} + c\dot{y} + ky = F_o \sin 2\pi f t. \tag{6.1}$$

The response curve for such a system is given in almost all standard text books on vibration, and indicates a significant response only for $f/f_N \approx 1$, with the response tending to zero for $f/f_N \gg 1$, as shown in figure 10(a), for finite damping ($c > 0$).

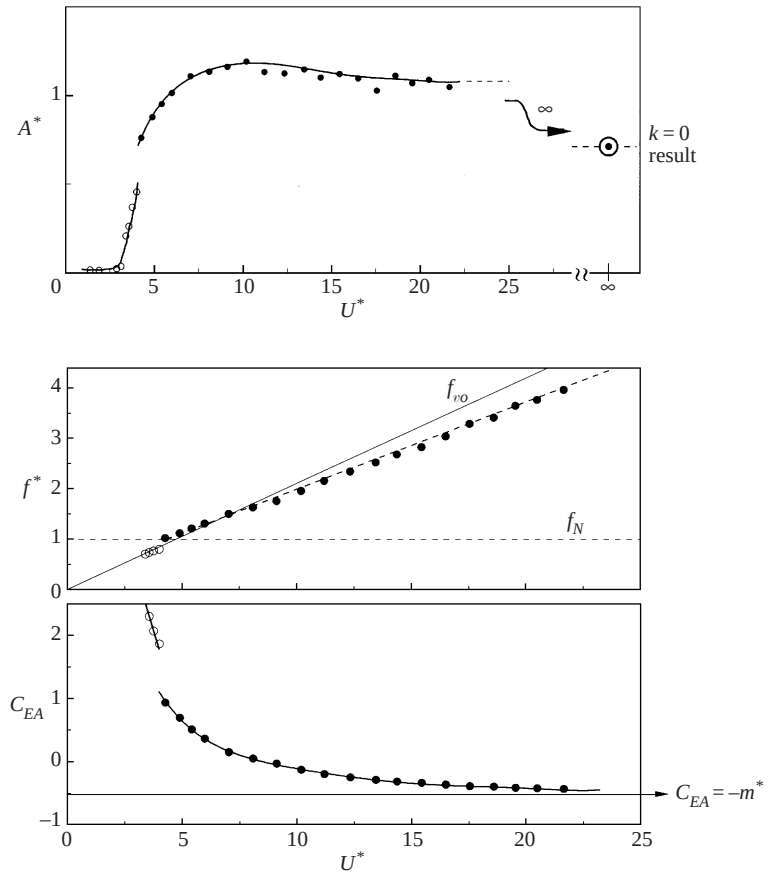

FIGURE 9. Response for $m^* < m^*_{crit}$, showing an infinite regime of 'resonance' (in this case, $m^* = 0.52$). The response amplitude at $U^* = \infty$, which corresponds to $k = 0$ experiments, remains large ($A^* \approx 0.7$). The frequency response ($f^* = f/f_N$) increases nearly linearly with U^* and tends to very large numbers, while the 'effective added mass' (C_{EA}) asymptotes towards the condition $C_{EA} = -m^*$, as $U^* \to \infty$. ○, the initial branch; ●, the upper branch; ⊙, the $k = 0$ experiments ($U^* = \infty$).

The response curve generally presented is actually the magnification factor (M) defined as

$$M = \frac{A}{A_{static}}, \tag{6.2}$$

where A is the response amplitude, and A_{static} is the static deflection under the force F_o and stiffness k. The parameter A_{static} has the form $A_{static} = F_o/k = F_o/(m4\pi^2 {f_N}^2)$.

In many practical and text book examples, the values $\{m, f_N, F_o\}$ are taken to be constants, and therefore the response shape of the factor M in figure 10(a) would represent the shape of response amplitude A, as a function of forcing frequency f. Therefore one is normally led to expect that amplitude drops off rapidly after $(f/f_N) \approx 1.0$, and asymptotes to zero for larger forcing frequencies. However, our case is clearly different.

Let us introduce the idea that F_o is no longer a constant, but varies as a function of (f/f_N), such that the amplitude asymptotes instead to a finite value, as frequency becomes large. Since M varies as $(f/f_N)^{-2}$ at large frequencies, F_o needs to vary

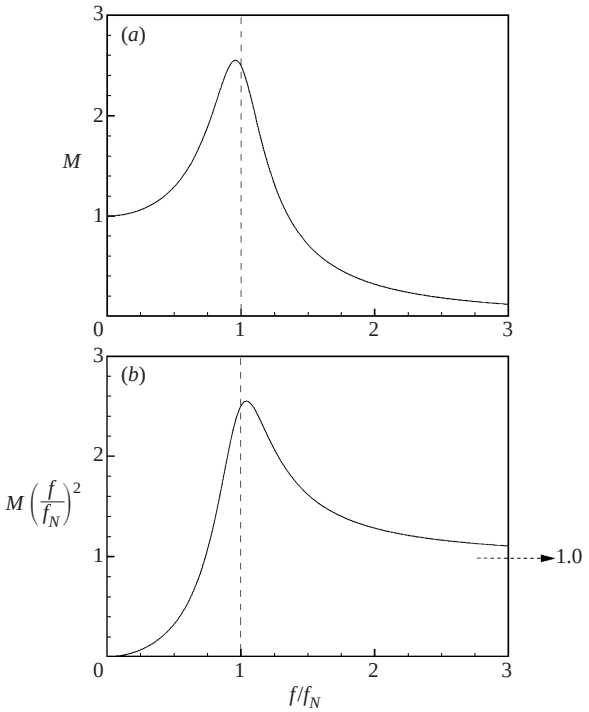

FIGURE 10. Variation of (a) magnification factor (M) and (b) $M(f/f_N)^2$ as a function of the frequency ratio (f/f_N).

as follows:

$$F_o \propto \left(\frac{f}{f_N}\right)^2 \tag{6.3}$$

and in this case the response amplitude is given by

$$A = \text{constant} \times M\left(\frac{f}{f_N}\right)^2. \tag{6.4}$$

We plot $M(f/f_N)^2$ as a function of the forcing frequency in figure 10(b). This response has a peak amplitude close to $(f/f_N) \approx 1.0$ as before, but now we see that it asymptotes to a finite value (1.0) as forcing frequency becomes large, and appears similar to the type of response we see in these experiments.

Let us now consider the present vortex-induced vibration system. As U^* becomes large, and for a given value of mass ratio (m^*) and damping (c), we approach very closely an 'operating point' in the plane $\{f_{vo}/f, A^*\}$. (Such an operating point is shown for example, by the $k = 0$ case in figures 6 and 7). This holds true for any given damping (c) or mass ratio (m^*). This means that for large U^*, significant variation in U^* results in practically no change of location in the frequency-amplitude plane, and one can consider the location as fixed at the operating point, and therefore to a good approximation

$$\left(\frac{f_{vo}}{f}\right) = \left(\frac{U^*}{f^*}\right) S = \text{constant} \tag{6.5a}$$

and thus,

$$U^* \propto f^*. \tag{6.5b}$$

Also, very close to the 'operating point', C_y will be constant, so that

$$F_o = (0.5\rho C_y DL)U^2, \tag{6.6a}$$

$$F_o \propto U^2. \tag{6.6b}$$

For a given natural frequency, f_N, and using equations (6.5*b*) and (6.6*b*):

$$F_o \propto \left(\frac{f}{f_N}\right)^2. \tag{6.7}$$

Thus, for our system the response A^*, at large velocities U^*, does indeed reach an asymptote, whose value is given by the amplitude of the operating point. The simple deductions laid out above, are not unexpected, and they follow naturally from the results presented in the paper. However, we may also consider that such phenomena will occur throughout a whole class of vortex-induced vibration problems.

In conclusion, such a large-amplitude 'resonant' response at very high normalized velocity (or very high forcing frequency) might be expected for any vortex-induced vibration system, which is well represented by such a linear forced oscillator, and where the forcing amplitude is proportional to the square of the forcing frequency.

7. Critical mass as a generic phenomenon in vortex-induced vibration

In this section, we shall define the critical mass ratio for a generic vortex-induced vibration system. Consider a system that is well represented by the simple mass–spring–dashpot:

$$m\ddot{y} + c\dot{y} + ky = F, \tag{7.1}$$

where m = oscillating mass, k = spring constant, c = damping coefficient, and F = fluid force. Here we shall also define the critical mass ratio (m^*_{crit}) to be the maximum mass ratio (m^* = mass/displaced mass) at which a large-amplitude synchronized response is possible at infinite non-dimensional flow speed ($U^* = U/f_N D = \infty$), for a given 'equivalent mass-damping' value.

It is important to note, in the general case, that the concept of an operating point in the frequency–amplitude plane, and the equations for its location that were derived in § 4, are valid for any body and not specific to the case of an oscillating cylinder. One would again interpret the operating point as being the intersection of the curves from both the amplitude equation and the frequency equation in the frequency–amplitude plane, in just the same way as we did for the vibrating cylinder. The dimensional form of the equations for the location of the operating point are exactly the same. In the general case, there can however be changes in the numerical values of the constants associated with the non-dimensional form of the amplitude equation (4.6) because of changes in the displaced volume of fluid and in the definition of C_y.

We now need to determine the maximum mass ratio at which a synchronized response is possible, in the case of an unrestrained body. From the frequency equation, which again takes the form $m^* = -C_{EA}$ in the general case, this would imply that the critical mass ratio (m^*_{crit}) will be given by the maximum value of $[-C_{EA}]$ that the vortex dynamics can provide, or

$$m^*_{crit} = \left[-\frac{1}{2\pi^3 A^* S^2}(f_{vo}/f)^2 C_y \cos\phi\right]_{max}, \tag{7.2}$$

where the maximum is taken over all the points on the amplitude curve, where there are synchronized vibrations of non-negligible amplitude.

Further, for a significant amplitude response to be seen at $U^* = \infty$ in a real physical experiment, we require $\phi > 90^\circ$ somewhere on the amplitude curve, in order that m^*_{crit} is a positive quantity. (Strictly speaking the condition is $90^\circ < \phi < 270^\circ$, but since positive energy transfer from the fluid to the body motion is possible only for $0 < \phi < 180^\circ$, the condition may be more simply written as $\phi > 90^\circ$.)

Therefore, for any generic vortex-induced vibration system that is well represented by a simple forced linear oscillator and where a synchronized response is found for $\phi > 90^\circ$, there will exist a critical mass ratio (m^*_{crit}) below which the regime of significant large-amplitude oscillations will extend to infinite velocity, U^*.

Apart from the present study of the transversely oscillating cylinder, we have also looked in particular at the dynamics of a sphere free to oscillate transverse to the flow direction (Govardhan & Williamson 2002), and we find a critical mass ratio, m^*_{crit}, of 0.30 for this case at low damping conditions.

8. Discussion of numerical simulations at low Reynolds numbers

The numerical study of Shiels *et al.* (2001) at low Reynolds numbers ($Re = 100$) investigated the response of a cylinder under a number of different conditions, one of which included zero spring constant ($k = 0$). It should be noted that the wake dynamics are markedly different at these low Re; for example the '2P' wake mode in figure 2(b) does not occur at these low Re. Nevertheless, we shall show that re-analysis of their original data also indicates the existence of a critical mass consistent with our present ideas, although the numbers are quite different in this regime of laminar vortex formation.

From the discussion in the previous sections, we know that the critical mass ratio (m^*_{crit}) is given by the relation, $m^*_{crit} = [-C_{EA}]_{max}$, where the maximum is taken over all the points in the frequency–amplitude plane that satisfy the amplitude equation. Therefore, to predict m^*_{crit} for the data of Shiels *et al.* (2001) under zero damping conditions, we need to find $[-C_{EA}]$ along a 'zero-excitation' contour deduced from their data. This can be calculated from their zero-damping response data by expressing their parameter k^*_{eff} in terms of the parameters used in the present study:

$$k^*_{eff} = \frac{2\pi^3 S^2}{(f_{vo}/f)^2} C_{EA}. \tag{8.1}$$

From tabulated values of k^*_{eff} and also $(fD/U) = [(f_{vo}/f)^{-1}S]$ in their paper, for the case where the spring constant (k) is greater than and equal to zero, C_{EA} values can be calculated using the above equations. The resulting C_{EA} values along the zero-excitation curve are shown in figure 11, predicting that $m^*_{crit} = [-C_{EA}]_{max} = 0.25$ for their low-Re study.

Direct measurement of the critical mass ratio from experiments with no springs ($k = 0$) in figure 12, confirm that the critical mass ratio, m^*_{crit} is indeed close to 0.25, which is consistent with our ideas of the concept of a critical mass.

9. Concluding remarks

In this paper, we study experimentally, for the first time, the transverse vortex-induced vibrations of a cylinder with no structural restoring force.

The present experiments indicate that a reduction of mass ratios m^* (mass/displaced mass) from the classically studied values of order $m^* = 100$, down to $m^* = 1$, yields

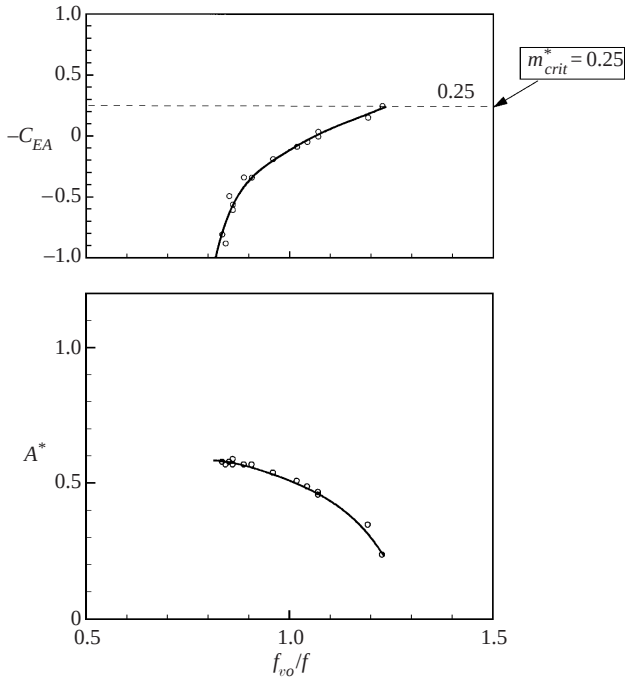

FIGURE 11. Amplitude and 'effective added mass' (C_{EA}), from $k > 0$ and $k = 0$ responses of the low Reynolds number numerical simulations of Shiels *et al.* (2001). The figure indicates that at these low *Re*, $m^*_{crit} = [-C_{EA}]_{max} \approx 0.25$.

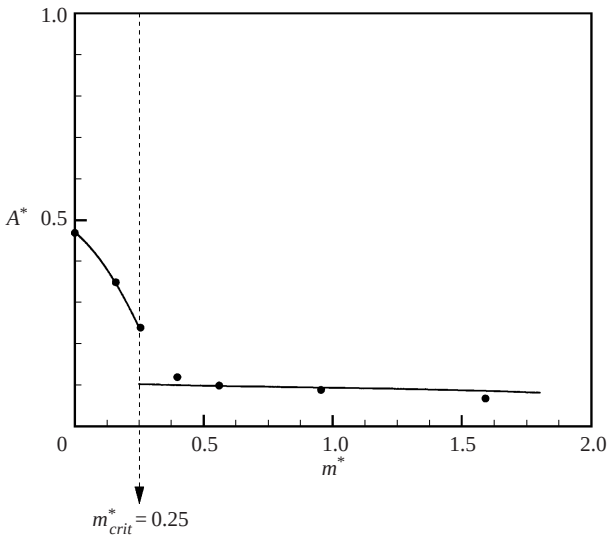

FIGURE 12. Amplitude response as a function of mass ratio, for $k = 0$ simulations of Shiels *et al.* (2001) for $Re = 100$, indicating the existence of a critical mass ratio (m^*_{crit}).

negligible oscillations. This is despite the fact that the cylinder is free to move and is being subjected to large transverse (lift) forces from the strong vortex shedding. However, a further reduction in mass exhibits a surprising result: large-amplitude vigorous vibrations suddenly appear for values of mass less than a critical mass ratio, $m^*_{crit} = 0.54$.

The response for such a system on a frequency–amplitude plane is found to be nearly independent of flow velocity (within the regime $Re = 4000$–$22\,000$), and we refer to such a response point as the *operating point*. The location of this operating point is found to be sensitive to variations in mass ratio; its precise position being principally dictated by the following equation:

$$-C_{EA} = m^*,$$

where C_{EA} is the effective added mass coefficient whose numerical value is defined by the wake vortex dynamics. From the above equation, it can be seen that for an unrestrained body of a given mass ratio, m^*,

if wake vortex dynamics can satisfy $-C_{EA} = m^*$
then the body will vibrate,
if wake vortex dynamics cannot satisfy $-C_{EA} = m^*$
then the body will NOT vibrate.

Measurements of $[-C_{EA}]$ from the spring-mounted cylinder experiments of Govardhan & Williamson (2000), indicate that the wake vortex dynamics give a value of $[-C_{EA}]_{max} = 0.54$, at small mass damping independent of the precise value of mass or damping. This implies that for a cylinder in the absence of springs ($k = 0$) and with small values of mass damping, the body will vibrate only if the chosen mass ratio, m^*, is less than 0.54. This value agrees remarkably well with the critical mass obtained from the present experiments without springs ($k = 0$):

$$m^*_{crit} = 0.542 \pm 0.01.$$

In terms of the conventionally used normalized flow velocity, $U^* = U/f_N D$ ($f_N =$ natural frequency, $D =$ diameter), the present experiments with $f_N = 0$, correspond to $U^* = \infty$. This proves that for $m^* < m^*_{crit}$, 'resonant' large-amplitude oscillations are possible at infinite U^*, as predicted by the spring-mounted cylinder studies of Govardhan & Williamson (2000). As flow velocities are increased from rest, resonance is initiated for a flow speed ($U^* \sim 5$) when the vortex formation frequency (and thereby the forcing frequency) is close to the natural frequency in water, i.e. when $f \sim f_N$. As velocities are further increased, the resonant large-amplitude oscillations persist up to infinite flow speeds; there is an infinitely wide regime of resonance, and in this sense, the *cylinder resonates forever*. The fact that we have an infinitely wide regime of resonance is in sharp contrast with the classical assumptions that resonant vibrations will exist only over a narrow regime of velocities, $U^* \sim 5$–8. Our result means also that oscillation frequencies can become large, $f \gg f_N$, which is again distinct from the often-used condition that $f \sim f_N$ for synchronization between forcing frequency and vibration frequency.

We should mention that the evaluation of critical mass ($m^*_{crit} = 0.54$), and also the response plots in this and previous work, seem to be independent of Reynolds number within the regime $Re = 4000$–$22\,000$. This seems reasonable since these results fall into the turbulent vortex shedding regime (for a fixed body) described in the reviews of Roshko (1993) and Williamson (1996). However, it is also expected that in the laminar vortex formation regime ($Re = 49$–190), where the response amplitudes, vortex formation modes, and Strouhal numbers are quite different from the turbulent shedding regime, one will find a numerically different evaluation of the critical mass. Indeed, from our analysis of the original data from the computed simulations by Shiels *et al.* (2001) at $Re = 100$, we deduce the critical mass to be: $m^*_{crit} = 0.25$.

Further, we deduce that for any vortex-induced vibration system that is well represented by a simple forced linear mass–spring–dashpot system, and where a synchronized response is found for phase angles ϕ greater than 90°, there will necessarily exist a critical mass ratio m^*_{crit}. When the mass of the vibrating system is below this value, the regime of large-amplitude 'resonant' response will extend to infinite flow speed, $U^* \to \infty$.

Evidence to date suggests that all of the vortex-induced vibration systems that we are studying in our laboratories exhibit a critical mass (whose value depends on the physical system); for example the critical mass ratio for an elastically mounted sphere is 0.30. On the basis of this work one might suggest that the existence of a critical mass is indeed a generic phenomenon in vortex-induced vibration.

The support from the Ocean Engineering Division of ONR, monitored by Dr Tom Swean, is gratefully acknowledged (ONR Contract Nos. N00014-94-1-1197 and N00014-95-1-0332).

Appendix. Characterizing structural damping in experiments without springs

The structural damping is usually characterized by the damping ratio (ζ), which is the ratio of the damping (c) to the critical damping ($c_c = 4\pi f_N m$), as defined in any vibration text book. In the case of a system without springs, like the present case, the natural frequency is zero, thus making the critical damping equal to zero and the damping ratio equal to infinity, for any non-zero dimensional damping. In this case, a more useful damping parameter is the non-dimensional damping term in the response amplitude equation (equation (4.5)), which we shall define here to be the equivalent damping ratio (ζ_{eq}):

$$\zeta_{eq} = \left[\frac{c}{4\pi f_{vo}(m + m_A)}\right]. \tag{A 1}$$

The only change in this parameter compared with the classical damping ratio is the use of the stationary-body vortex shedding frequency (f_{vo}), instead of the natural frequency (f_N). (It should be noted that the potential added mass (m_A) is present in the damping term above only because the critical damping value is taken for the body in the fluid, as opposed to the body in vacuum.)

In the present experiments with no springs, the damping (c) was very small because of the use of air-bearings, and this resulted in very small equivalent damping ratios which ranged from $\zeta_{eq} = 0.001$ to 0.005. The combined mass-damping parameter, which is based here on ζ_{eq}, ranged from $(m^* + C_A)\zeta_{eq} = 0.002$ to 0.01. These values of mass damping are very low, and therefore correspond to the range of mass damping $[(m^* + C_A)\zeta < 0.1]$ where the effective added mass (C_{EA}) of the 'lower' branch, as discussed in Govardhan & Williamson (2000), remains constant at 0.54, independent of the precise mass or damping values.

REFERENCES

Bearman, P. W. 1984 Vortex shedding from oscillating bluff bodies. *Annu. Rev. Fluid Mech.* **16**, 195–222.

Carberry, J., Govardhan, R., Sheridan, J., Rockwell, D. & Williamson, C. H. K. 2002 Wake states and response branches of forced and freely oscillating cylinders. Submitted to the *Bluff Body Wakes and Vortex-induced Vibration* (*BBVIV3*) *Conference, Port Douglas, Queensland, Australia, December 2002.*

Gopalkrishnan, R. 1993 Vortex-induced forces on oscillating bluff cylinders. PhD Thesis, MIT, Cambridge, MA, USA.

Govardhan, R. & Williamson, C. H. K. 2000 Modes of vortex formation and frequency response of a freely vibrating cylinder. *J. Fluid Mech.* **420**, 85–130.

Govardhan, R. & Williamson, C. H. K. 2002 Vortex-induced vibrations of a sphere. To be submitted to *J. Fluid Mech.*

den Hartog, J. P. 1934 *Mechanical Vibrations.* Dover.

Hover, F. S., Techet, A. H. & Triantafyllou, M. S. 1998 Forces on oscillating uniform and tapered cylinders in crossflow. *J. Fluid Mech.* **363**, 97–114.

Khalak, A. & Williamson, C. H. K. 1996 Dynamics of a hydroelastic cylinder with very low mass and damping. *J. Fluids Struct.* **10**, 455–472.

Khalak, A. & Williamson, C. H. K. 1999 Motions, forces and mode transitions in vortex-induced vibrations at low mass-damping. *J. Fluids Struct.* **13**, 813–851.

Parkinson, G. 1989 Phenomena and modelling of flow-induced vibrations of bluff bodies. *Prog. Aerospace Sci.* **26**, 169–224.

Roshko, A. 1993 Perspectives on bluff body aerodynamics. *J. Wind Ind. Aerodyn.* **49**, 79–100.

Sarpkaya, T. 1979 Vortex-induced oscillations. *Trans. ASME J. Appl. Mech.* **46**, 241–258.

Shiels, D., Leonard, A. & Roshko, A. 2001 Flow-induced vibration of a circular cylinder at limiting structural parameters. *J. Fluids Struct.* **15**, 3–21.

Williamson, C. H. K. 1996 Vortex dynamics in the cylinder wake. *Annu. Rev. Fluid Mech.* **28**, 477–539.

Williamson, C. H. K. & Roshko, A. 1988 Vortex formation in the wake of an oscillating cylinder. *J. Fluids Struct.* **2**, 355–381.